JETIR.ORG ISSN: 2349-5162 | ESTD Year : 2014 | Monthly Issue
JOURNAL OF EMERGING TECHNOLOGIES AND INNOVATIVE RESEARCH (JETIR)
An International Scholarly Open Access, Peer-reviewed, Refereed Journal

Design of Sparrow Search Algorithm with Deep Transfer Learning-based Classification Model for Medical X-Ray Image Classification Model

[1]T. Kumar, [2]R. Ponnusamy

[1]Research Scholar, Department of Computer and Information Science, Annamalai University, Annamalai Nagar.

[2]Assistant Professor, Department of Computer and Information Science, Annamalai University, Annamalai Nagar.

Abstract

Medical Image diagnosis has dramatically improved during recent years. It can be a comparatively easy task to identify and diagnose chest X-ray (CXR) images however, the difficulty of the images sometimes provides inappropriate diagnosis. Subsequently, the achievement of deep learning (DL) in numerous industries, it has also confirmed outcomes in the form of superior accuracies for medical imaging. CXR image has a moderately inexpensive and available analytical tool, which must be supported in the analysis of different conditions, comprising COVID-19, pneumonia, tuberculosis, and others. Nevertheless, the necessity for practiced radiologists to evaluate and interpret CXR images should be a bottleneck, particularly in remote and deprived fields. New developments in machine learning (ML) are accomplished potential the automatic diagnosis of CXR images. This article develops a new Sparrow Search Algorithm with Deep Transfer Learning-based Medical X-ray Image Classification (SSADTL-MIC) technique, which is an innovative framework to increase the efficiency and accuracy of medical X-ray image classification. Leveraging the powerful EfficientNet as a feature extractor, the model ensures optimal representation learning from X-ray images, capturing intricate patterns and features critical for accurate diagnosis. The Sparrow Search Algorithm (SSA) is employed for hyperparameter tuning, utilizing the algorithm's optimization capabilities to fine-tune the model parameters and achieve superior performance. The proposed SSADTL-MIC technique introduces a novel approach by incorporating Long Short-Term Memory (LSTM) networks for the final classification stage. Through extensive experimentation, the SSADTL-MIC technique demonstrates superior performance compared to traditional systems.

Keywords: Chest X-Ray; Medical Image Classification; Deep Learning; Hyperparameter Tuning; Computer-Aided Diagnosis

1. Introduction

The Medical image analysis is a complex task for medical specialists to create sufficient usage of their knowledge, skill and imaging methods [1]. The automatic technique for irregularity detection in the medical X-ray image has a complicated issue in the machine learning (ML) domain. It has extensive anatomical variabilities in all patients.

Consequently, it is major significant problems in radiograph prediction that comprises superimposed structures [2]. The radiologists involve practical experience and skill to analyze X-ray images for the fracture identification at the bone [3]. The medical image with quality taken by image capturing tool can be reduced quality therefore, it is difficult for the physician for identifying the irregularity and a proficient automatic computer-aided detection (CAD) technique has been developed to address the issue [4]. Accordingly, the automatic deformity diagnosis of X-ray images supports the radiologist for analyzing numerous medical problems namely dental decay arthritis, osteoporosis, bone cancer, infection and fracture [5].

Chest X-ray (CXR) imaging is a most extensively employed medical imaging methods to identify and diagnose diseases, comprising COVID-19, malignancy, pneumonia, tuberculosis, and so on [6]. Its excessive benefit exists in its comparatively simple operation, higher availability, and lower-cost. Significant data about a patient's health could be extracted in CXR imaging as well as detection and manual analysis by CXR image marks and systems of diseases has been achieved by practiced radiologists [7]. Analyses are challenging and it is an extended and complex manner. Furthermore, the need for skilled radiologists has a bottleneck, particularly in remote or deprived field [8]. In order to overcome this difficulty, current study has considered the utilization of ML approaches for automatic analysis, with different techniques that achieving popularity as well as targeting to develop a main tool for medical practitioners. The cutting-edge expansion of medical image analysis methods, general-purpose graphics processing unit (GPU) hardware, and deep learning (DL) algorithms, which can be permitted researchers for automatically identifying diseases employing CXR image, and developing robust CAD methods [9]. The capability obtained from automatic X-ray analysis has improved automation of difficult day-to-day activities, sensitivity for outcomes, hierarchy of time-sensitive conditions, and resolving the problem of radiologists, which are not continually accessible in developing nations or remote regions [10]. CXR imaging has also comparatively inexpensive and available, with advanced digital radiographic machines becoming reasonable still, in under-developed nations.

2. Related Works

Loey et al. [11] aim of this study was classified CXR imaging of COVID19 objects in altered real-time conditions. An innovative Bayesian optimization (BO)-based CNNs method has been developed for identifying CXR images. This presented technique can be a 2 major constituents. The primary one employs CNN for removing and learning deep features. The secondary module is a BO that was applied for tuning the CNN hyperparameters in accordance with an objective task. Gopatoti and Vijayalakshmi [12] designed a tri-phase CXR image based COVID19 classification method employing DL-CNN with an optimum feature selection (FS) algorithm called as improved grey-wolf optimization with GA (EGWO-GA) that could be represented as CXGNet. Asif et al. [13] intended to automatically identify COVID19 pneumonia cases employing digital CXR images whereas improving the precision in identification by implementing deep-CNNs (DCNNs). DCNN based architecture like Inception-V3 with transfer learning (TL) must be presented for recognizing COVID19 pneumonia diseased patients through CXR images. In [14], a DCNN framework was designed in this work for diagnosing COVID19 dependent upon the CXR image classification. An efficient and precise CNN classification can be a problem because of the non-accessibility of adequate size and better quality CXR image database.

In [15], the authors established how pre-trained DL method was implemented for executing COVID-19 identification employing CXR images. The goal is to offer overworked diagnosticians another pair of eyes via intelligent image classification methods. The authors emphasize the problems (containing quality and dataset size) in employing existing openly accessible COVID-19 databases for emerging beneficial DL techniques. The authors developed a semi-automatic image preprocessing system for making a reliable image database in designing and testing DL methods. In [16], the authors employed numerous ML methods for categorizing the bone X-ray images of MURA database such as two types such as no fracture and fractures. A 4 diverse methods linear SVM, LBF-SVM (Radial Basis Function (RBF), support vector machine), Decision tree (DT) and Logistic Regression (LR) could be implemented to detect abnormalities.

This article develops a new Sparrow Search Algorithm with Deep Transfer Learning-based Medical X-ray Image Classification (SSADTL-MIC) technique, which is an innovative framework to increase the accuracy and proficiency of medical X-ray image classification. Initially, the SSADTL-MIC technique was applied EfficientNet model as a feature extractor. Moreover, the Sparrow Search Algorithm (SSA) is employed for hyperparameter tuning, utilizing the algorithm's optimization capabilities to fine-tune the model parameters and achieve superior performance. Finally, the SSADTL-MIC technique introduces a novel approach by incorporating Long Short-Term Memory (LSTM) networks for classification stage. Through extensive experimentation, the SSADTL-MIC technique demonstrates superior performance compared to traditional methods.

3. The Proposed Model

In this article, we develop a new SSADTL-MIC technique, which is an innovative framework to enhance the efficiency and accuracy of medical X-ray image classification. The proposed SSADTL-MIC technique contains three major processes namely EfficientNet based feature extractor, SSA based hyperparameter tuning, and LSTM based classification. Fig. 1 depicts the workflow of SSADTL-MIC technique.

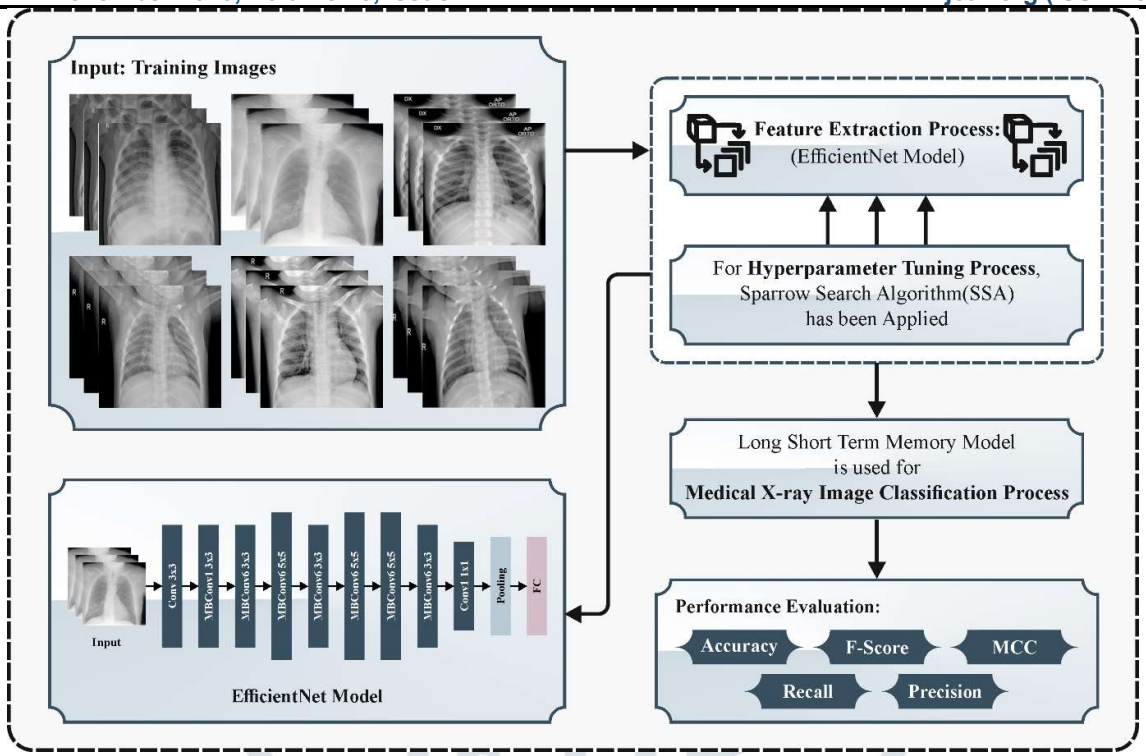

Fig. 1. Workflow of SSADTL-MIC technique

3.1. EfficientNet feature extractor

Initially, the SSADTL-MIC technique applied EfficientNet model as a feature extractor. EfficientNet can be a category of CNNs architectures especially designed for obtaining advanced performance in image classification even though increasing model size as well as computational efficiency [17]. It offers an innovative scaling method that consistently calculates network resolution, depth, and width to determine an optimal balance amongst these sizes. The major notion behind EfficientNet was intricate scaling that analytically increases both depth and width to be provide enriched representation capacity as well as better generalization. Additionally, it predicts an original complex scaling coefficient signified as φ that describes scaling factor for all dimensions. By proficiently measuring these sizes, EfficientNet gets better performance with some parameters and computational requirements while related to other CNNs. EfficientNet methods developed for offering remarkable precision on diverse benchmark databases, which must be extremely proper for applications like image recognition and object detection. These attacks are a major balance among predictive power and computational efficiency that makes them primarily attractive for resource-limited conditions namely mobile devices and edge computing. This proficiency is frequently attributed to their aptitude to optimize feature representation while decreasing model's complete difficulty which is exceptionally vital for implementing DL outcomes in real-time situations with limited computational resources.

3.2. SSA based hyperparameter tuning

At this stage, the SSA-based hyperparameter tuning can be implemented to fine-tune the model parameters and achieve superior performance. SSA is a new optimization approach based on the collaborative and migratory behaviors of a salp swarm, and resolves optimization difficulties by simulating the behavior [18]. Every bottlenose sea squirt is calculated after initializing the population for fitness and chain based on its fitness values. The

highest-rated bottlenose sea squirts in the chain should be known as leaders, and the residual part has been called as followers.

They update the position based on dissimilar principles, and location x_j^i of leader can be improved by the following expression.

$$x_j^i = \begin{cases} F_j + c_1\left(\left(ub_j - lb_j\right) \cdot c_2 + lb_j\right) & c_3 \geq 0 \\ F_j - c_1\left(\left(ub_j - lb_j\right) \cdot c_2 + lb_j\right) & c_3 < 0' \end{cases} \tag{1}$$

In Eq. (1), the location of food source at j^{th} dimension is F_j; ub_j and lb_j are the upper and lower bounds of the jth dimension; and c_1, c_2, and c_3 are randomly generated values.

The updating of follower's location has been rented from the concept of Newtonian motion and represents shown below.

$$x_j^i = \frac{1}{2}at^2 + v_0 t,$$
$$a = \frac{v_{final}}{v_0}, \tag{2}$$
$$v = \frac{x - x_0}{t}.$$

For $i \geq 2$ represents the location of ith follower bottle sea squirt at t denote the time, and j^{th} dimension. v denotes the velocity whereby v_0 and v_{final} indicates the initial and the last velocity, x and x_0 shows the present as well as initial locations, correspondingly. This pseudocode for SSA is given in Algorithm 1.

Algorithm 1: Salp Swarm Algorithm (SSA)

```
Input: ub, lb
Output: fitness
xi ←initial population considering ub and lb
Function SSA ()
 While ending criteria is not met do
    Compute the fitness of search agent (salp)
      Set F as the food source
      For each salp (x)do
        If the salp population is in the top half then
          Update the location of leading salp based on Eq. (1)
        Else
          Update the location of follower salp based on Eq. (2)
        End if
      End for
    End while
```

```
        Return F
End function
```

The interaction and movement of virtual sheath in the search range provides a stronger global search ability; then, diverse features of SSA make it execute better in handing multi-peak optimizer issues that fits to search for the optimum workload distribution system.

The fitness selection is the significant aspect prompting the effectiveness of the SSA method. The hyperparameter selection procedure includes the solution encoding technique for determining the efficiency of candidate solutions. The SSA model deliberates accurateness as the main condition to develop the FF that must be expressed as given below.

$$Fitness = \max(P) \tag{3}$$

$$P = \frac{TP}{TP + FP} \tag{4}$$

Where, FP denotes the false positive and TP represent the true positive value.

3.3. Classification using LSTM model

Finally, the SSADTL-MIC technique introduces a novel approach by incorporating LSTM networks for classification stage. LSTM is a branch of DL. It falls below recurrent neural networks (RNNs) and then well-known for its capability to hold longer-term addictions mainly and contains sequence prediction [19]. It takes an input and then spreads it to others. LSTM's cells execute the wide range of challenges. Moreover, LSTM contains memory state which able to recall data as well as learn longer term addictions for lengthened epochs. As an outcome, LSTMs is said to be valued device in several fields namely time-series forecast, speech recognition and natural language processor.

LSTM has a major benefit than RNN that is it includes a cell state in order to hoard longer period information. This permits data from earlier time phases to be reserved as well as associated in present time step in LSTM. To attain this, LSTM uses 3 gates such as forget, output and input gate. The current input represented as i_t, whereas C_t and C_{t-1} signify present and previous cell states, correspondingly. Also, H_t and H_{t-1} denotes previous and current output, respectively. Fig. 2 represents the infrastructure of LSTM.

LSTM layer receives opinion from layer of dropout. A calculation fabricated of 4 portions like input gate (i_t), forget gate, an output gate and a novel memory container. To incorporate act of forward as well as backward, an element-wise calculation considered depend on Eqs. (5)-(8):

An LSTM takes a present input a preceding state(h_{t-1}) performs few calculation on Eqs. (5)-(8) and then links information in preparation of hidden state$(\vec{h})$ as mentioned:

$$f_t = \sigma\left(U_f h_{t-1}, W_f X_\tau + b_f\right) \tag{5}$$

$$i_t = \sigma\left(U_i h_{t-1}, W_i X_t + b_f\right) \tag{6}$$

$$a_t = tanh(U_c h_{t-1}, W_c X_t + b_c)$$

$$= tan(\hat{a}_t) \tag{7}$$

$$o_t = \sigma(U_o h_{t-1}, W_o X_t + b_o) \tag{8}$$

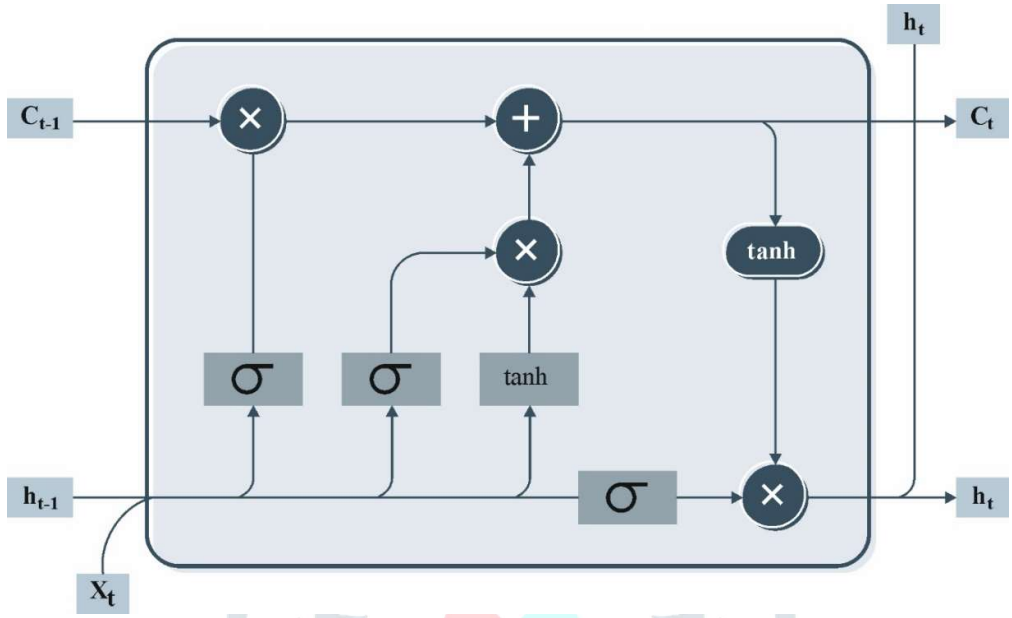

Fig. 2. LSTM structure

4. Results and Discussion

In this section, the X-ray image classification analysis of the SSADTL-MIC method can be validated under the X-ray image database in the Kaggle repository [20]. The dataset includes 3000 instances with 3 classes as described in Table 1.

Table 1 Details of dataset

Class	**No. of Images**
COVID	1000
Normal	1000
Viral Pneumonia	1000
Total No. of Instances	**1000**

Fig. 3 displays the classifier outcomes of the SSADTL-MIC system on 80:20 of TRPH/TSPH. Figs. 3a-3b shows the confusion matrices acquired by the SSADTL-MIC technique. This figure exhibits that the SSADTL-MIC algorithm can be correctly identified and categorized with 3 classes. Additionally, Fig. 3c reveals the PR analysis of the SSADTL-MIC system. This figure described the SSADTL-MIC method gets great PR performance with all classes. Also, Fig. 3d represents the ROC analysis of the SSADTL-MIC algorithm. The figure revealed the SSADTL-MIC model offers proficient outcomes with higher ROC values with diverse classes.

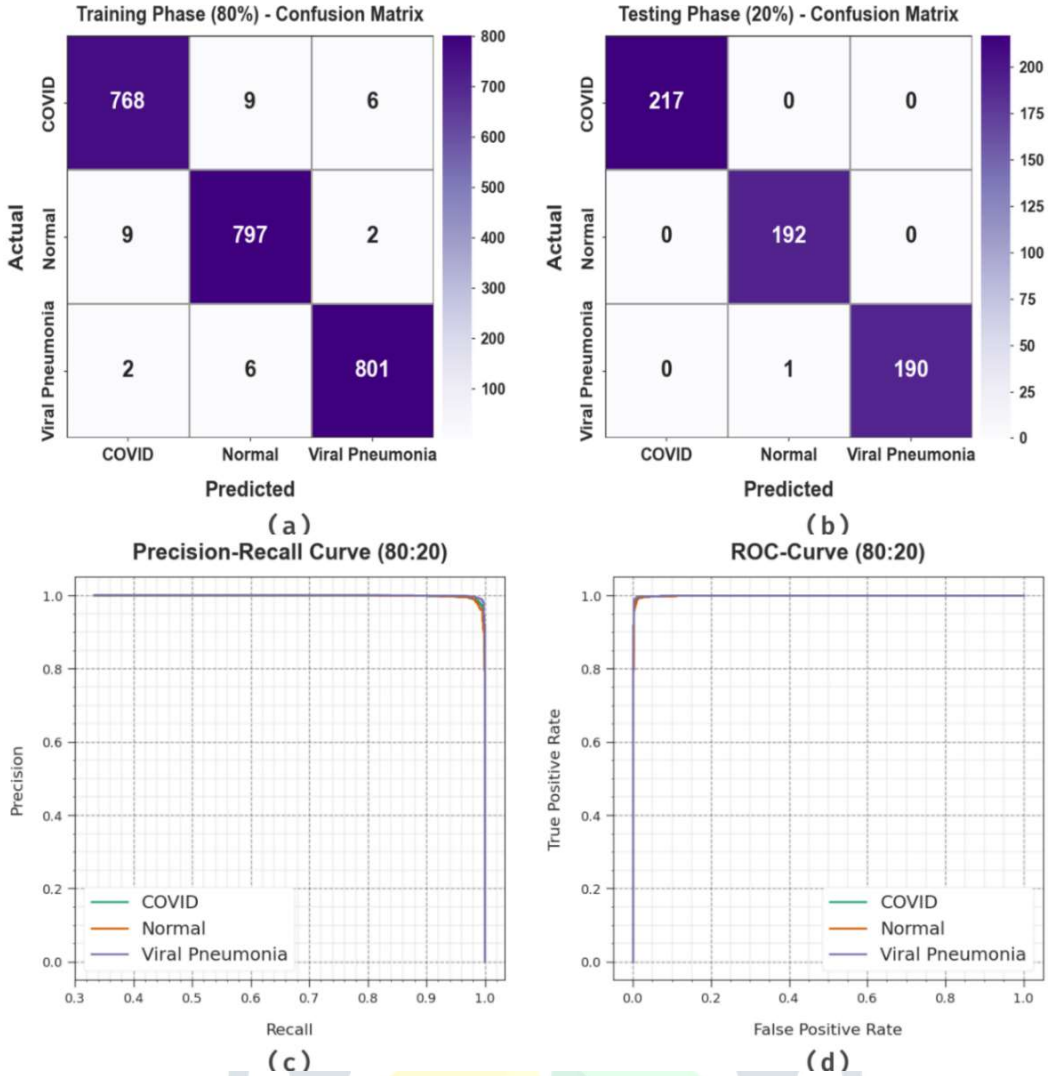

Fig. 3. 80:20 of TRPH/TSPH (a-b) Confusion matrices and (c-d) PR and ROC curves

In Table 2, a comprehensive X-ray image classification analysis of the SSADTL-MIC method with 80:20 of TRPH/TSPH can be confirmed. The figure displayed that the SSADTL-MIC method acquires better performance with 3 classes. According to 80% of TRPH, the SSADTL-MIC method achieves average $accu_y$ of 99.06%, $prec_n$ of 98.58%, $reca_l$ of 98.58%, F_{score} of 98.58%, and MCC of 97.87%. Meanwhile, on 20% of TSPH, the SSADTL-MIC technique gets average $accu_y$ of 99.89%, $prec_n$ of 99.83%, $reca_l$ of 99.83%, F_{score} of 99.83%, and MCC of 99.71%.

Table 2 Classifier analysis of SSADTL-MIC model with 80:20 of TRPH/TSPH

Class	$Accu_y$	$Prec_n$	$Reca_l$	F_{score}	MCC
TRPH (80%)					
COVID	98.92	98.59	98.08	98.34	97.53
Normal	98.92	98.15	98.64	98.40	97.58
Viral Pneumonia	99.33	99.01	99.01	99.01	98.51
Average	**99.06**	**98.58**	**98.58**	**98.58**	**97.87**
TSPH (20%)					
COVID	100.00	100.00	100.00	100.00	100.00
Normal	99.83	99.48	100.00	99.74	99.62
Viral Pneumonia	99.83	100.00	99.48	99.74	99.62
Average	**99.89**	**99.83**	**99.83**	**99.83**	**99.74**

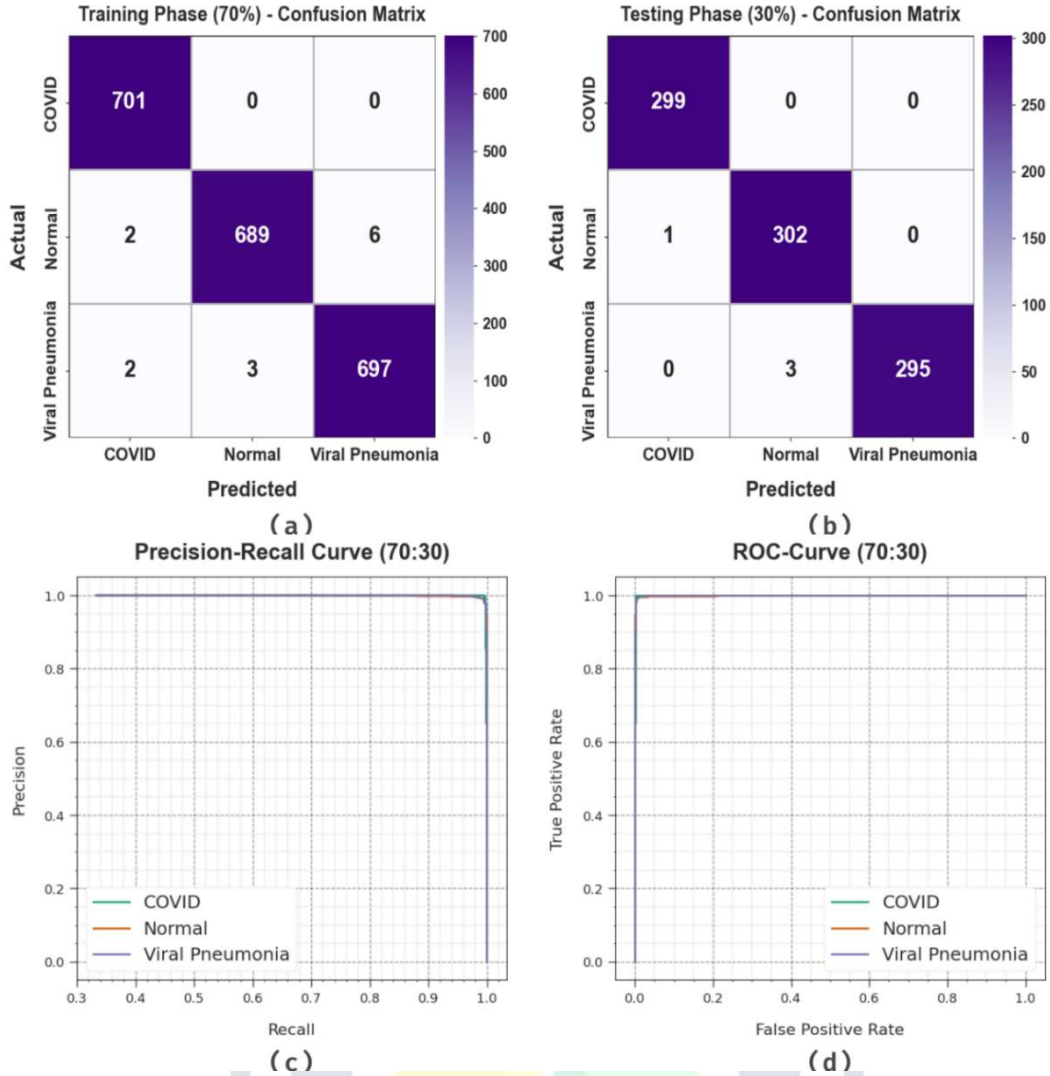

Fig. 4. 70:30 of TRPH/TSPH (a-b) Confusion matrices and (c-d) PR and ROC curves

Fig. 4 illustrates the classifier analysis of the SSADTL-MIC technique in 70:30 of TRPH/TSPH. Figs. 4a-4b represented the confusion matrices obtained by the SSADTL-MIC algorithm. The figure signified that the SSADTL-MIC methodology can be precisely identified and categorized with 3 class labels. Moreover, Fig. 4c exhibits the PR analysis of the SSADTL-MIC system. The figure shows the SSADTL-MIC system obtains great PR performance with each class. Next, Fig. 4d demonstrates the ROC analysis of the SSADTL-MIC algorithm. This figure exposed that the SSADTL-MIC methodology provides efficient outcomes with superior ROC values with numerous classes.

In Table 3, a wide-ranging X-ray image classification analysis of the SSADTL-MIC method with 70:30 of TRPH/TSPH has been revealed. This figure shows the SSADTL-MIC method gets increased performance on 3 classes. Based on 70% of TRPH, the SSADTL-MIC approach gains average $accu_y$ of 99.59%, $prec_n$ of 99.38%, $reca_l$ of 99.38%, F_{score} of 99.38%, and MCC of 99.07%. Then, with 30% of TSPH, the SSADTL-MIC system acquires average $accu_y$ of 99.70%, $prec_n$ of 99.56%, $reca_l$ of 99.55%, F_{score} of 99.56%, and MCC of 99.34% respectively.

Table 3 Classifier outcome of SSADTL-MIC system with 70:30 of TRPH/TSPH

Class	$Accu_y$	$Prec_n$	$Reca_l$	F_{score}	MCC
TRPH (70%)					
COVID	99.81	99.43	100.00	99.72	99.57
Normal	99.48	99.57	98.85	99.21	98.82
Viral Pneumonia	99.48	99.15	99.29	99.22	98.82
Average	**99.59**	**99.38**	**99.38**	**99.38**	**99.07**
TSPH (30%)					
COVID	99.89	99.67	100.00	99.83	99.75
Normal	99.56	99.02	99.67	99.34	99.01
Viral Pneumonia	99.67	100.00	98.99	99.49	99.25
Average	**99.70**	**99.56**	**99.55**	**99.56**	**99.34**

Table 4 and Fig. 5 displays the comparison analysis of SSADTL-MIC system with other existing methodologies [21, 22]. The accomplished outcome revealed that the SSADTL-MIC method can be proficient outcome with compared to others approaches. According to $accu_y$, the SSADTL-MIC method obtains boosting $accu_y$ of 99.89% while the SqueezeNet, TLSqueezeNet, VGG19, TLResNet2, and ResNet1 techniques get lower $accu_y$ values of 92.96%, 96.44%, 93.30%, 98.44%, and 97.23%.

Table 4 Comparison analysis of SSADTL-MIC technique with other methods

Methods	$Accu_y$	$Prec_n$	$Reca_l$
SqueezeNet	92.96	91.73	95.10
TLSqueezeNet	96.44	96.08	96.84
VGG19 Model	93.30	91.78	94.73
TLResNet2	98.44	97.97	97.94
ResNet1 Model	97.23	96.74	97.43
SSADTL-MIC	99.89	99.83	99.83

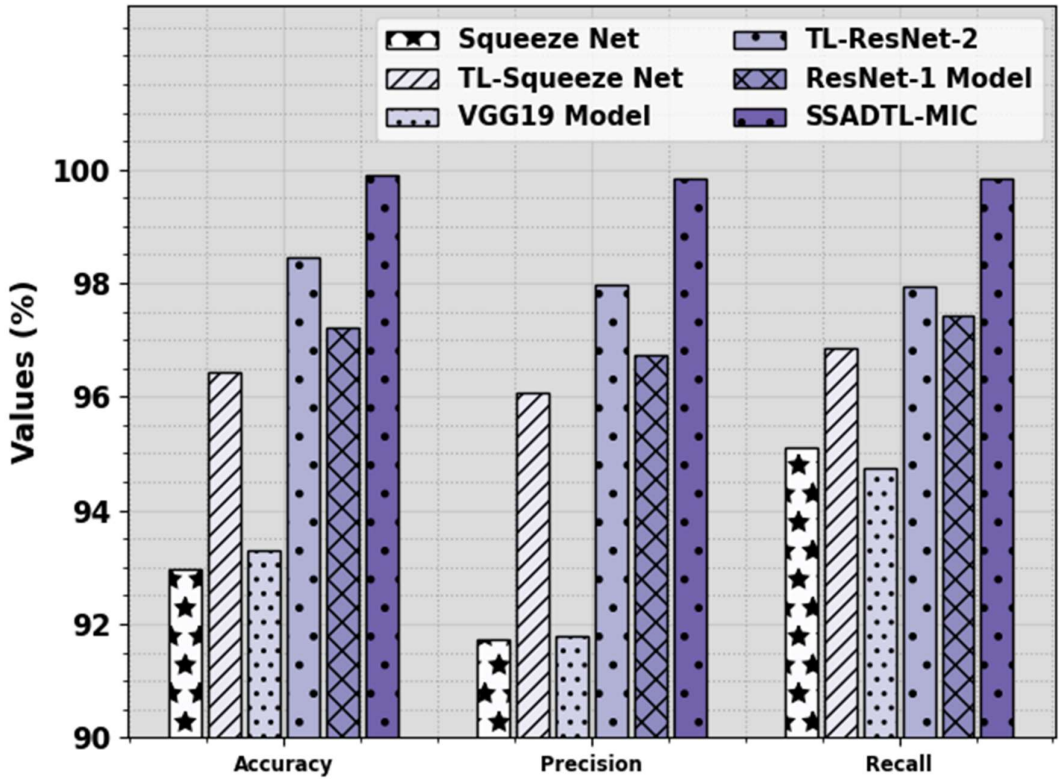

Fig. 5. Comparative analysis of SSADTL-MIC technique with other methods

Furthermore, with $reca_l$, the SSADTL-MIC system gains increasing $reca_l$ of 99.83% whereas the SqueezeNet, TLSqueezeNet, VGG19, TLResNet2, and ResNet1 methods obtain reduced $reca_l$ values of 95.10%, 96.84%, 94.73%, 97.94% and 99.83% correspondingly. These results confirmed the enhanced performance of the proposed models over existing models.

5. Conclusion

In this article, we develop a new SSADTL-MIC technique, which is an innovative framework to increase the accuracy and efficiency of medical X-ray image classification. The proposed SSADTL-MIC technique contains three major processes namely EfficientNet-based feature extractor, SSA based hyperparameter tuning, and LSTM based classification. Initially, the SSADTL-MIC method was applied EfficientNet model as a feature extractor. Moreover, the SSA-based hyperparameter tuning is utilized to fine-tune the model parameters and achieve superior performance. Finally, the proposed SSADTL-MIC technique introduces a novel approach by incorporating LSTM networks for classification stage. Through extensive experimentation, the SSADTL-MIC technique demonstrates superior performance compared to traditional methods.

References

[1] Tiu, E., Talius, E., Patel, P., Langlotz, C.P., Ng, A.Y. and Rajpurkar, P., 2022. Expert-level detection of pathologies from unannotated chest X-ray images via self-supervised learning. *Nature Biomedical Engineering*, pp.1-8.

[2] Awan, M.J., Bilal, M.H., Yasin, A., Nobanee, H., Khan, N.S. and Zain, A.M., 2021. Detection of COVID-19 in chest X-ray images: A big data enabled deep learning approach. *International journal of environmental research and public health*, *18*(19), p.10147.

[3] Constantinou, M., Exarchos, T., Vrahatis, A.G. and Vlamos, P., 2023. COVID-19 classification on chest X-ray images using deep learning methods. *International Journal of Environmental Research and Public Health*, *20*(3), p.2035.

[4] Sirazitdinov, I., Kholiavchenko, M., Mustafaev, T., Yixuan, Y., Kuleev, R. and Ibragimov, B., 2019. Deep neural network ensemble for pneumonia localization from a large-scale chest x-ray database. *Computers & electrical engineering*, *78*, pp.388-399.

[5] Moussaid, A., Zrira, N., Benmiloud, I., Farahat, Z., Karmoun, Y., Benzidia, Y., Mouline, S., El Abdi, B., Bourkadi, J.E. and Ngote, N., 2023, February. On the Implementation of a Post-Pandemic Deep Learning Algorithm Based on a Hybrid CT-Scan/X-ray Images Classification Applied to Pneumonia Categories. In *Healthcare* (Vol. 11, No. 5, p. 662). MDPI.

[6] Guan, Q. and Huang, Y., 2020. Multi-label chest X-ray image classification via category-wise residual attention learning. *Pattern Recognition Letters*, *130*, pp.259-266.

[7] Jakaite, L., Schetinin, V., Hladůvka, J., Minaev, S., Ambia, A. and Krzanowski, W., 2021. Deep learning for early detection of pathological changes in x-ray bone microstructures: case of osteoarthritis. *Scientific Reports*, *11*(1), pp.1-9.

[8] Zouch, W., Sagga, D., Echtioui, A., Khemakhem, R., Ghorbel, M., Mhiri, C. and Hamida, A.B., 2022. Detection of COVID-19 from CT and chest X-ray images using deep learning models. *Annals of Biomedical Engineering*, *50*(7), pp.825-835.

[9] Keidar, D., Yaron, D., Goldstein, E., Shachar, Y., Blass, A., Charbinsky, L., Aharony, I., Lifshitz, L., Lumelsky, D., Neeman, Z. and Mizrachi, M., 2021. COVID-19 classification of X-ray images using deep neural networks. *European radiology*, *31*(12), pp.9654-9663.

[10] Jin, Y., Lu, H., Zhu, W. and Huo, W., 2023. Deep learning based classification of multi-label chest X-ray images via dual-weighted metric loss. *Computers in Biology and Medicine*, *157*, p.106683.

[11] Loey, M., El-Sappagh, S. and Mirjalili, S., 2022. Bayesian-based optimized deep learning model to detect COVID-19 patients using chest X-ray image data. *Computers in Biology and Medicine*, *142*, p.105213.

[12] Gopatoti, A. and Vijayalakshmi, P., 2022. CXGNet: A tri-phase chest X-ray image classification for COVID-19 diagnosis using deep CNN with enhanced grey-wolf optimizer. *Biomedical Signal Processing and Control*, *77*, p.103860.

[13] Asif, S., Wenhui, Y., Jin, H. and Jinhai, S., 2020, December. Classification of COVID-19 from chest X-ray images using deep convolutional neural network. In *2020 IEEE 6th international conference on computer and communications (ICCC)* (pp. 426-433). IEEE.

[14] Reshi, A.A., Rustam, F., Mehmood, A., Alhossan, A., Alrabiah, Z., Ahmad, A., Alsuwailem, H. and Choi, G.S., 2021. An efficient CNN model for COVID-19 disease detection based on X-ray image classification. *Complexity*, *2021*, pp.1-12.

[15] Horry, M.J., Chakraborty, S., Paul, M., Ulhaq, A., Pradhan, B., Saha, M. and Shukla, N., 2020. X-ray image based COVID-19 detection using pre-trained deep learning models.

[16] Mall, P.K., Singh, P.K. and Yadav, D., 2019, December. GLCM based feature extraction and medical X-RAY image classification using machine learning techniques. In *2019 IEEE Conference on Information and Communication Technology* (pp. 1-6). IEEE.

[17] Chowdhury, N.K., Kabir, M.A., Rahman, M.M. and Rezoana, N., 2020. ECOVNet: an ensemble of deep convolutional neural networks based on EfficientNet to detect COVID-19 from chest X-rays. *arXiv preprint arXiv:2009.11850*.

[18] Cai, W. and Duan, F., 2023. Task Scheduling for Federated Learning in Edge Cloud Computing Environments by Using Adaptive-Greedy Dingo Optimization Algorithm and Binary Salp Swarm Algorithm. *Future Internet*, *15*(11), p.357.

[19] Nasser, A.A., Rashad, M.Z. and Hussein, S.E., 2020. A two-layer water demand prediction system in urban areas based on micro-services and LSTM neural networks. *IEEE Access*, *8*, pp.147647-147661.

[20] https://www.kaggle.com/tawsifurrahman/covid19-radiography-database

[21] Khan, S.H., Sohail, A., Khan, A., Hassan, M., Lee, Y.S., Alam, J., Basit, A. and Zubair, S., 2021. COVID-19 detection in chest X-ray images using deep boosted hybrid learning. *Computers in Biology and Medicine*, *137*, p.104816.

[22] Ragab, M., Alshehri, S., Alhakamy, N.A., Alsaggaf, W., Alhadrami, H.A. and Alyami, J., 2022. Machine Learning with Quantum Seagull Optimization Model for COVID-19 Chest X-Ray Image Classification. *Journal of Healthcare Engineering*, *2022*.